Moment-Method Analysis of Arbitrary 3-D Metallic N-Port Waveguide Structures

Rainer Bunger, *Member, IEEE*, and Fritz Arndt, *Fellow, IEEE*

***Abstract*—Moment-method analysis of arbitrarily shaped perfectly conducting ("metallic") waveguide structures with N waveguide ports is presented that is based on the free-space Green's function. Utilizing the Kirchhoff–Huygens principle, the problem is formulated in terms of the electric-field integral equation. The eigenvectors of the waveguide port sections and the Rao–Wilton–Glisson functions for triangular patches are used as basis functions for the magnetic and electric surface current densities, respectively. The accuracy of the method is verified by measurements or reference values. Its versatility is demonstrated at several design examples of practical interest, such as a lateral coax-fed waveguide, a twisted waveguide, and a waffle-iron filter with round teeth.**

***Index Terms*—CAD, method of moments, waveguide discontinuities, waveguide filters, waveguide junctions.**

I. Introduction

MOMENT-METHOD [1] solutions of waveguide discontinuity problems have been widely studied in the past and applied to many practical examples, such as irises, obstacles, probes, and septa in waveguides [2]–[7]. The utilization of the eigenfunctions of the waveguide structure under consideration for the Green's function in these approaches automatically meets the boundary conditions, but restricts, on the other side, the solutions to this specific waveguide structure type.

This paper describes a new moment-method analysis for arbitrarily shaped three–dimensional (3-D) metallic N-port waveguide structures [cf. Fig. 1(a)]. Based on the Green's functions for the potentials in free space, the advantage of the method is its high flexibility.

The accuracy of the method is verified by measurements at a post compensated T-junction, as well as a structure with two crossed posts, and by reference calculations. Its versatility is demonstrated at several design examples of practical interest.

II. Theory

The entire structure to be investigated is subdivided into two regions [8], [9]: regions I and II [cf. e.g., Fig. 1(b)]. Region I is further subdivided into N subregions corresponding to N waveguides connected to the general N-port waveguide structure: region II. Both regions are separated by a perfectly conducting surface S_a, where $S_a = S_a^1 + \cdots + S_a^N$. In order to maintain the original problem, magnetic surface current densities are introduced in the usual way, which restore the tangential electric field on the surface S_a.

Enforcing the continuity of the tangential magnetic field on the aperture surface S_a yields the following equation:

$$\mathbf{H}_{\tan}^{\text{inc}} = \mathbf{H}_{\tan}^{I}(\mathbf{M}) + \mathbf{H}_{\tan}^{II}(\mathbf{M}), \qquad \text{on } S_a \tag{1}$$

where $\mathbf{M}$ is the magnetic surface current density, and $\mathbf{H}_{\tan}^{\text{inc}}$, $\mathbf{H}_{\tan}^{I}(\mathbf{M})$, and $\mathbf{H}_{\tan}^{II}(\mathbf{M})$ are the tangential incident magnetic field in region I, the linear operator for the tangential scattered magnetic field in region I and the linear operator for the tangential scattered magnetic field in region II, respectively [8], [9]. The field $\mathbf{H}_{\tan}^{I}(\mathbf{M})$ is generated by the magnetic surface current density $-\mathbf{M}$ placed inside region I on the perfectly conducting surface S_a. $\mathbf{H}_{\tan}^{II}(\mathbf{M})$ is the field caused by the magnetic surface current density $\mathbf{M}$ placed inside region II on S_a and radiating in presence of the perfectly conducting surface S_b of the 3-D waveguide structure.

A. Region I

For the solution of (1), the method of moments is employed. The magnetic surface current density is approximated by Q linear independent basis functions $\mathbf{M}_q$ on the aperture surface S_a

$$\mathbf{M}(\mathbf{r}) = \eta_0 \sum_{q=1}^{Q} V_q \mathbf{M}_q(\mathbf{r}), \qquad \mathbf{r} \text{ on } S_a \tag{2}$$

where V_q are the expansion coefficients for the magnetic surface current density to be determined on the N apertures, and η_0 denotes the free-space wave impedance. Introducing a set of $P = Q$ linear independent test functions $\mathbf{W}_p$ on S_a results in a system of linear equations

$$\left[I_{pj}^{\text{inc}}\right] = \left[T_{pq}^{I} + T_{pq}^{II}\right]\left[V_{qj}\right] \tag{3a}$$

with the excitation matrix

$$\left[I_{pj}^{\text{inc}}\right] = \left[\left\langle \mathbf{W}_p; \mathbf{H}_{\tan}^{\text{inc},j} \right\rangle\right] \tag{3b}$$

the admittance matrices for regions I and II

$$\left[T_{pq}^{I}\right] = \left[\eta_0 \left\langle \mathbf{W}_p; \mathbf{H}_{\tan}^{I}(\mathbf{M}_q) \right\rangle\right] \tag{3c}$$

$$\left[T_{pq}^{II}\right] = \left[\eta_0 \left\langle \mathbf{W}_p; \mathbf{H}_{\tan}^{II}(\mathbf{M}_q) \right\rangle\right] \tag{3d}$$

Manuscript received November 24, 1998.

The authors are with the Microwave Department, University of Bremen, D-28334 Bremen, Germany.

Publisher Item Identifier S 0018-9480(00)02769-1.

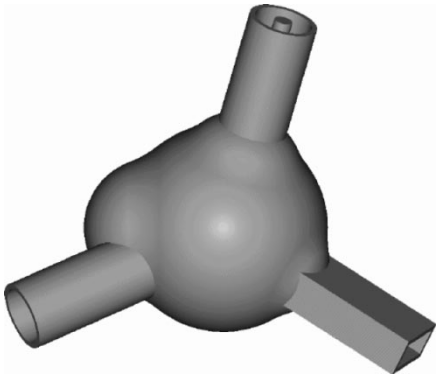

(a)

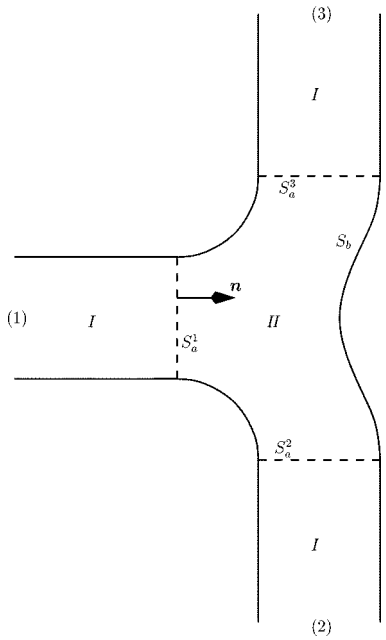

(b)

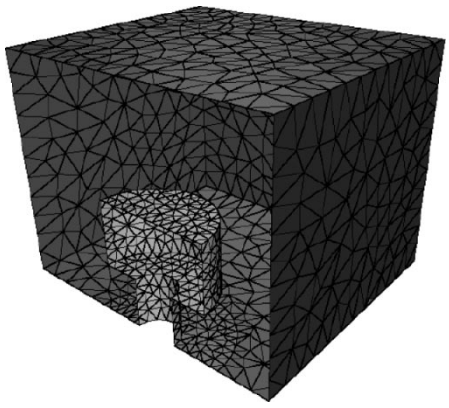

(c)

Fig. 1. (a) Arbitrary 3-D metallic waveguide structure with N waveguide ports. (b) Regions I, II, separated by a perfectly conducting surface S_a, where $S_a = S_a^1 + \cdots + S_a^N$. (c) Discretization of an example: Lateral coax-fed rectangular waveguide.

and the inner products defined as

$$\langle \mathbf{A}; \mathbf{B} \rangle = \int_S \mathbf{A} \cdot \mathbf{B}\, dS. \tag{3e}$$

The index j denotes the excitation by a mode j guided by waveguide n.

The elements of the waveguide admittance matrix for region I and the excitation matrix are elucidated in the Appendix.

B. Region II

The calculation of the N-port admittance matrix for the arbitrarily shaped metallic 3-D waveguide structure II is based on the Kirchhoff–Huygens principle [10], [11]. The electromagnetic field in region II is calculated using the magnetic surface current densities on S_a and the electric surface current densities on S_a and S_b

$$\mathbf{M}(\mathbf{r}) = \begin{cases} -\mathbf{n} \times \mathbf{E}(\mathbf{r}), & \mathbf{r} \text{ on } S_a \\ 0, & \mathbf{r} \text{ on } S_b, \end{cases} \tag{4a}$$

$$\mathbf{J}(\mathbf{r}) = \mathbf{n} \times \mathbf{H}(\mathbf{r}), \qquad \mathbf{r} \text{ on } S_a \text{ or } S_b. \tag{4b}$$

The electromagnetic field in region II can be written as

$$\mathbf{E}(\mathbf{r}) = -\mathrm{rot} \int_S \mathbf{M}(\mathbf{r}') G_0(\mathbf{r}, \mathbf{r}')\, dS' + \frac{1}{j\omega\epsilon_0} \mathrm{rot}\,\mathrm{rot} \int_S \mathbf{J}(\mathbf{r}') G_0(\mathbf{r}, \mathbf{r}')\, dS' \tag{5a}$$

$$\mathbf{H}(\mathbf{r}) = \mathrm{rot} \int_S \mathbf{J}(\mathbf{r}') G_0(\mathbf{r}, \mathbf{r}')\, dS' + \frac{1}{j\omega\mu_0} \mathrm{rot}\,\mathrm{rot} \int_S \mathbf{M}(\mathbf{r}') G_0(\mathbf{r}, \mathbf{r}')\, dS' \tag{5b}$$

with the Green's function for the potentials in free space

$$G_0(\mathbf{r}, \mathbf{r}') = \frac{1}{4\pi} \frac{e^{-jk_0|\mathbf{r}-\mathbf{r}'|}}{|\mathbf{r}-\mathbf{r}'|} \tag{5c}$$

and where a time dependence of $e^{j\omega t}$ is understood. The calculations in this paper are based on (5a), for reasons that are elucidated in Section III-A.

The magnetic and electric surface current densities are approximated by (2) and

$$\mathbf{J}(\mathbf{r}) = \sum_{s=1}^{S} I_s \mathbf{J}_s(\mathbf{r}), \qquad \mathbf{r} \text{ on } S_a \text{ and } S_b \tag{6}$$

respectively, where the electric surface current density is approximated by S linear independent basis functions $\mathbf{J}_s$ on the surfaces S_a and S_b.

The electric and magnetic surface current densities in (5a) are replaced by the approximations (2) and (6). The tangential fields on the surfaces S_a and S_b are related with the corresponding surface current densities via (4a) and (4b). After introducing a set of R linear independent test functions $\mathbf{U}_r$ on S_a and S_b, writing inner products of $\mathbf{U}_r$ and (5a), a system of linear equations results as follows:

$$\left[D_{rq}^M\right][V_q] = \left[S_{rq}^M\right][V_q] + \left[T_{rs}^J\right][I_s] \tag{7a}$$

with

$$S_{rq}^{M} = \left\langle \mathbf{U}_r; -\mathrm{rot} \int_{S_a} \mathbf{M}_q \, G_0 \, dS' \right\rangle \tag{7b}$$

$$T_{rs}^{J} = \frac{1}{jk_0} \left\langle \mathbf{U}_r; \mathrm{rot}\,\mathrm{rot} \int_{S_a+S_b} \mathbf{J}_s \, G_0 \, dS' \right\rangle \tag{7c}$$

$$D_{rq}^{M} = \langle \mathbf{U}_r; \mathbf{n} \times \mathbf{M}_q \rangle \tag{7d}$$

where we have omitted the arguments for the sake of a more compact notation. Vectors $[V_q]$ and $[I_s]$ denote the column of the corresponding matrices for a excitation by the mode j. The system of linear equations (7a) can be solved for the current vector $[I_s]$

$$[I_s] = \left[T_{rs}^{J}\right]^{-1} \left[D_{rq}^{M} - S_{rq}^{M}\right] \left[V_q\right] \tag{8}$$

Now utilizing the linearity of the operator $\mathbf{H}^{II}$ and (4b), the following expression can be derived:

$$\eta_0 \sum_{q=1}^{Q} V_q \left\langle \mathbf{W}_p; \mathbf{H}_{\tan}^{II}(\mathbf{M}_q) \right\rangle = \sum_{s=1}^{S} I_s \langle \mathbf{W}_p; -\mathbf{n} \times \mathbf{J}_s \rangle, \quad p = 1, \cdots, P. \tag{9}$$

Introducing the matrix

$$\left[F_{ps}^{J}\right] = \left[\langle \mathbf{W}_p; -\mathbf{n} \times \mathbf{J}_s \rangle\right] \tag{10}$$

equation (9) can be written in the matrix form

$$\left[T_{pq}^{II}\right] \left[V_q\right] = \left[F_{ps}^{J}\right] [I_s]. \tag{11}$$

From this equation and (8), the expression for the admittance matrix for region II results as follows:

$$\left[T_{pq}^{II}\right] = \left[F_{ps}^{J}\right] \left[T_{rs}^{J}\right]^{-1} \left[D_{rq}^{M} - S_{rq}^{M}\right]. \tag{12}$$

C. Calculation of the Scattering Matrix

Using the orthonormality of the eigenvectors, the following expression for the elements of the modal scattering matrix is obtained:

$$s_{ij} = -\eta_0 \sum_{q} A_{iq} V_{qj} - \delta_{ij}. \tag{13}$$

In deriving this equation, it has been assumed that every incident mode is of an amplitude equal to one. The summation index q considers all basis functions q on the aperture of the waveguide, which is associated with the mode i. As already mentioned above, the jth column of $[V_{qj}]$ is the vector of the Q expansion coefficients for the magnetic surface current density for a excitation with mode j only.

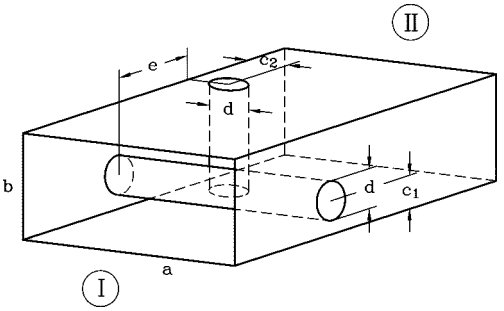

(a)

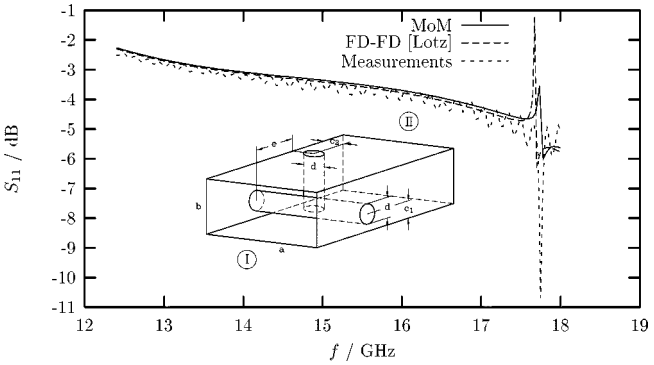

(b)

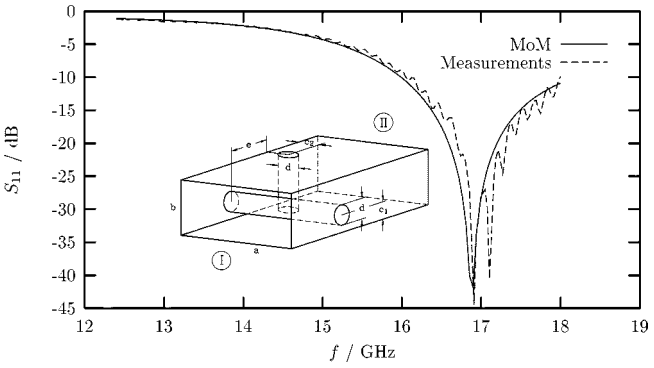

(c)

Fig. 2. (a) Two crossed posts. Dimensions: $a = 15.7988$ mm, $b = 7.8994$ mm, $c_1 = 2.5$ mm, $c_2 = 4.0$ mm, $d = 3.0$ mm, $e = 5.0$ mm. (b) Two crossed posts, $e = 5.0$ mm. Scattering parameter S_{11} over frequency. (c) Two crossed posts, $e = 11.51$ mm. Scattering parameter, S_{11} over frequency.

III. Implementation

A. Choice of the Basis Functions and Test Functions

Own investigations and those in [12]–[14] have shown that the choice of basis functions for the electric and magnetic surface current densities is critical. The use of the Rao–Wilton–Glisson (RWG) triangular basis functions $\mathbf{f}$ [15] for *both* the electric *and* magnetic surface current densities would result in a numerically singular matrix $[T^{I} + T^{II}]$.

A more illustrative explanation of this fact may be the observation that the electric field given by the first term on the right-hand side of (5a), if caused by an RWG basis function for the magnetic surface current density, would not be "well tested" by an RWG test function (see also [14]). The numerical evaluation of the corresponding S-matrix integrals in (7b) requires

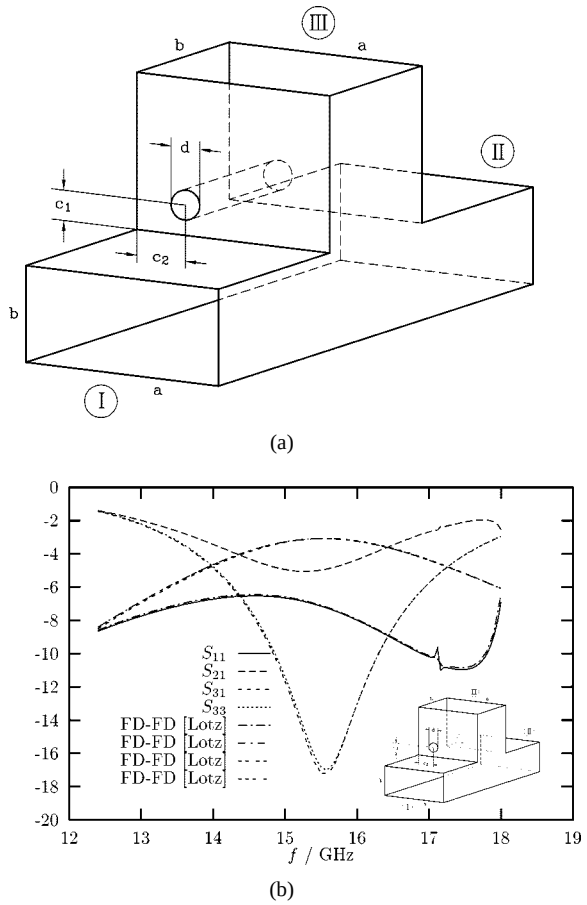

Fig. 3. (a) Tee with post. Dimensions: $a = 15.7988$ mm, $b = 7.8994$ mm, $c_1 = 2.5$ mm, $c_2 = 4.0$ mm, $d = 3.0$ mm. (b) Tee with post. Scattering parameters over frequency.

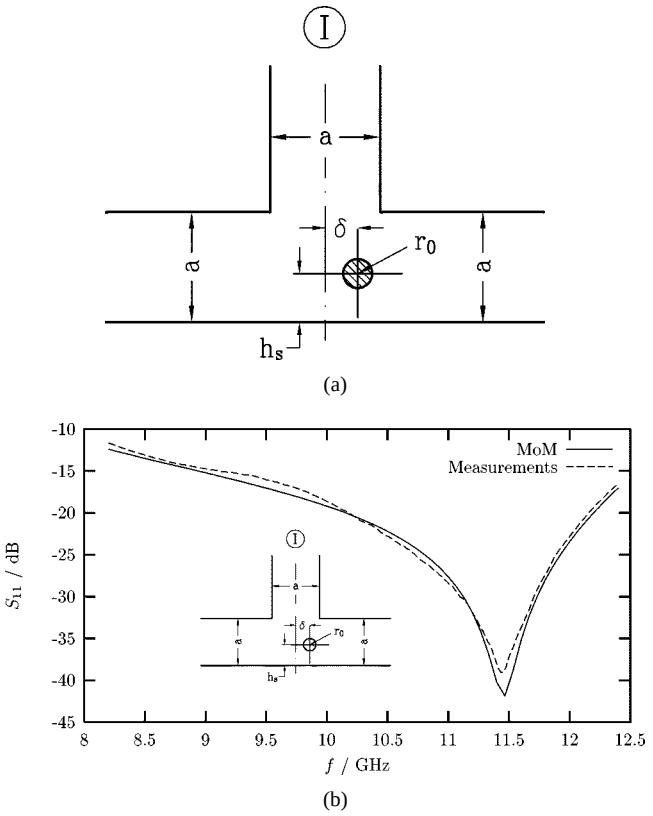

Fig. 4. (a) Tee with post. Dimensions: $a = 22.86$ mm, $\delta = 0.1$ mm, $h_s = 8.8$ mm, $r_0 = 0.75$ mm. (b) Tee with post. Scattering parameters S_{11} over frequency.

the separation into a Cauchy principal value term and a residue term in the well-known way[1] as follows:

$$\mathrm{rot}\int_S \mathbf{M}_q(\mathbf{r}')G_0(\mathbf{r},\mathbf{r}')dS' = -\frac{1}{2}\mathbf{n}\times\mathbf{M}_q(\mathbf{r}) + \mathrm{rot}\oint_S \mathbf{M}_q(\mathbf{r}')G_0(\mathbf{r},\mathbf{r}')\,dS'. \tag{14}$$

For the case $r = q$ (self-coupling), the first term on the right-hand side of this expression gives the main contribution to the integral on the left-hand side, which is (with an additional negative sign) the electric field caused by a basis function for the magnetic surface current density. This term is tested out to zero when using RWG functions for both the basis and test functions in (7b).

Therefore, the $-\mathbf{u}_z \times \mathbf{e}_i$ are chosen as basis functions for the magnetic surface current density. Due to their orthonormality, the admittance matrix $[T^I]$ and the incident current vectors $[I^{\mathrm{inc}}]$ are given analytically. Moreover, usually the number of columns of the matrices $[S^M]$ and $[D^M]$ is advantageously small.

[1]The expression is derived using a limiting process $\mathbf{r} \to \mathbf{r}'$ for the expression with the rot-operator under the integral sign.

When applying the magnetic-field integral equation (MFIE), which may be derived from (5b), a selection of RWG basis functions in the form $\mathbf{n} \times \mathbf{f}$ for the electric surface current densities seems to be appropriate. However, because of the $\mathbf{n}\times$ operation required for the RWG basis functions, their usual physically skillful attributes vanish. This set no longer meets the boundary conditions for the electric surface current density on open surfaces automatically, and it produces line charges. Therefore, the electric-field integral equation (EFIE) is preferred for the calculations in this paper. See [14] for further discussions concerning the choice of basis and test functions.

As for the test functions according to the chosen Galerkin Method, the $P = Q$ functions $\mathbf{W}_p$ are the basis functions for the magnetic surface current density $\mathbf{M}_q$; the $R = S$ functions $\mathbf{U}_r$ are those for the electric surface current density $\mathbf{J}_s$.

Symmetry walls are utilized in order to reduce memory and central processing unit (CPU) time requirements. For the corresponding implementation, every basis function is supplemented with additional images of itself.

B. Evaluation of the Moment-Method Integrals

The T-matrix elements are transformed into the well-known mixed potential form in order to have merely a $1/R$ singularity. The singularities are integrated analytically, e.g., with the help of the formulas developed in [16]. The remaining numerical integrations are evaluated in normalized area coordinates [15] using a three- and a seven-point rule [17].

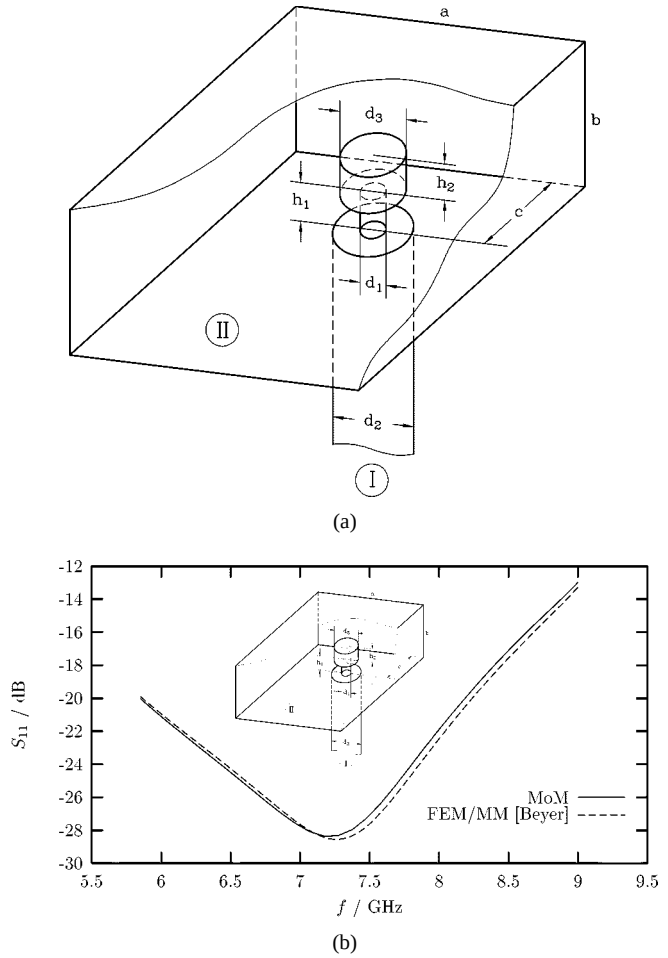

Fig. 5. (a) Coax-feed for a rectangular waveguide. Dimensions: $a = 34.8488$ mm, $b = 15.7988$ mm, $c = 11.6$ mm, $d_1 = 2 \times 1.5240$ mm, $d_2 = 2 \times 4.8768$ mm, $d_3 = 2 \times 4.0$ mm, $h_1 = 3.4$ mm, $h_2 = 4.5$ mm. (b) Coax-feed of a rectangular waveguide. Scattering parameter S_{11} over frequency.

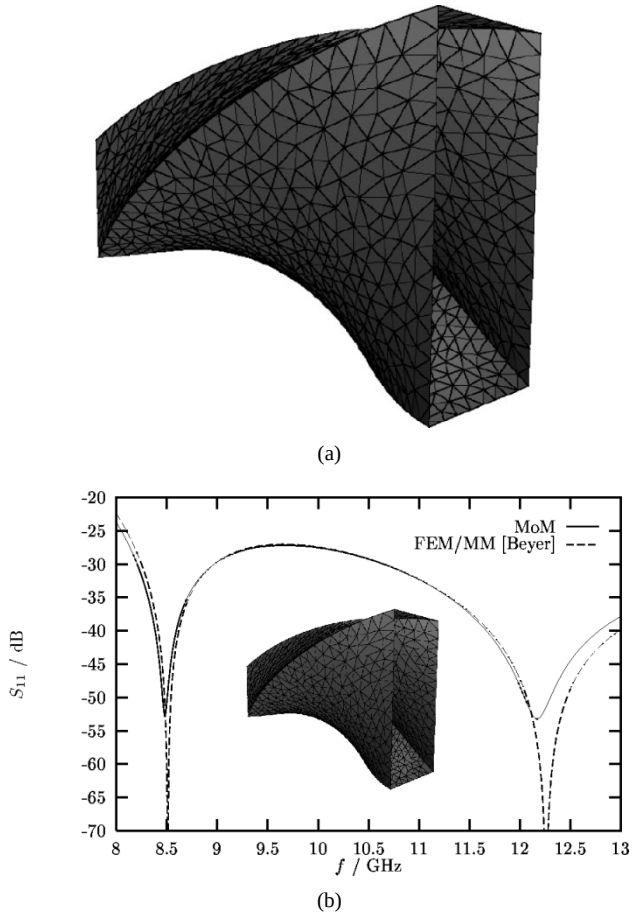

Fig. 6. (a) 90°-twisted waveguide. Dimensions of the rectangular waveguide cross section: $a = 22.86$ mm, $b = 10.16$ mm. Length of the structure: $l = 31.75$ mm. (b) Scattering parameter S_{11} of the twisted waveguide of Fig. 6(a).

The correct evaluation of the S-matrix elements requires the separation of the source point integral into a Cauchy principal value term and a residue term in the usual way (see also Section III-A).

IV. Results

For verification purposes, three examples are calculated (Figs. 2–4) where measurements are available. Fig. 2(a) shows two crossed metal posts in a WR-62 waveguide. The input return loss for different post distances $e = 5.0$ mm [see Fig. 2(b)] and $e = 11.51$ mm [see Fig. 2(c)] demonstrates good agreement with measurements and own finite-difference frequency-domain (FD–FD) calculations as reference values, respectively.

An E-plane T-junction with a post in the side port is shown in Fig. 3(a). The rather fast convergence of the method can be demonstrated by the fact that, e.g., for this example, only 12 modes, 36 triangular patches for each port waveguide cross section and 400 patches for the metallic surfaces have turned out to be sufficient. Already this low number of modes and this rather coarse grid yield scattering parameters, which show merely deviations in the order of a fraction of a decibel [see Fig. 3(b)] as compared with FD–FD reference values. For the FD–FD calculations, a subgrid technique [21] has been applied with an adequately fine subgrid level for convergent results.

A post in the main waveguide of an H-plane T-junction [see Fig. 4(a)] yields a broad-band compensation of the side-port return loss [18]. Such structures are advantageous, e.g., as a combiner for diplexer applications. Good agreement with measurements is demonstrated in Fig. 4(b).

Fig. 5(a) shows the example of a lateral coax feed for a rectangular waveguide. The discretization using triangular RWG patches of one-half of this structure and its apertures is illustrated in Fig. 1(c). The return loss in Fig. 5(b) demonstrates good agreement with reference calculations by a finite-element mode-matching method [19].

A triangular mesh describing a twisted WR-90 waveguide is given in Fig. 6(a). The scattering parameters shown in Fig. 6(b) are compared with reference values of a hybrid finite-element mode-matching method [19] using a staircase approximation with 60 steps.

The versatility of the presented method is demonstrated by the design example of a WR-650 waffle-iron filter with round teeth [see Fig. 7(a) and (b)]. For the initial filter dimensions, the values given in [20] have been chosen. The distance to the port waveguide of height 8.89 mm [20] and the lengths between the teeth rows have been optimized for a return loss of better than

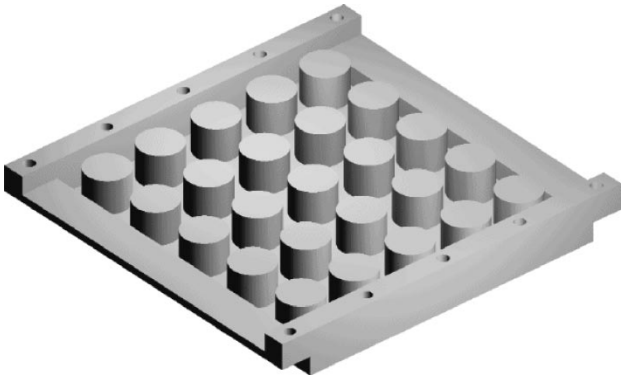

(a)

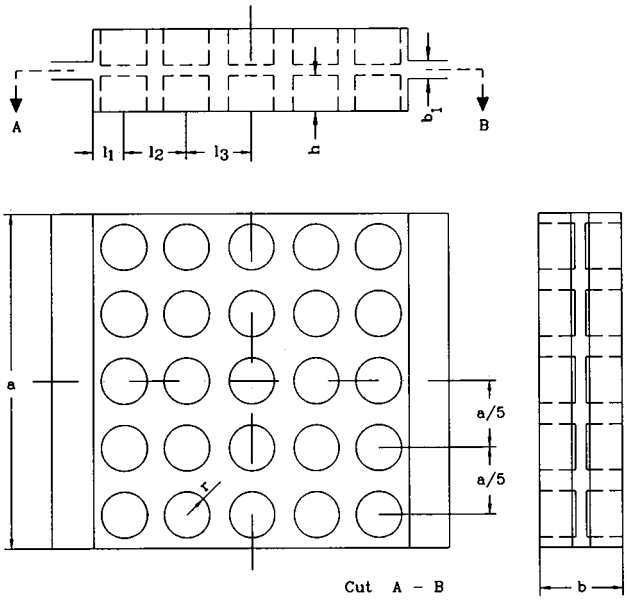

(b)

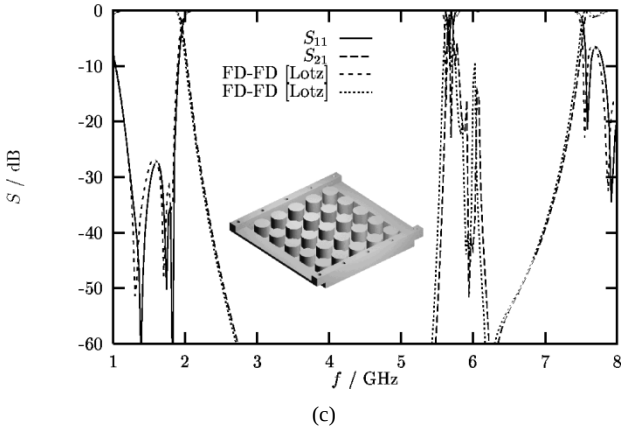

(c)

Fig. 7. (a) Waffle-iron filter with round teeth. (b) Waffle-iron filter with round teeth. Dimensions: $a = 165.1$ mm, $b = 40.894$ mm, $b_1 = 8.89$ mm, $l_1 = 15.1182$ mm, $l_2 = 31.0174$ mm, $l_3 = 32.5328$ mm, $r = 11.3411$ mm, $h = 17.78$ mm. (c) Scattering parameters of the waffle-iron filter of Fig. 7(b).

26 dB. The scattering parameters are presented in Fig. 7(c). The reliability of the method is demonstrated by comparison of the results (solid lines) with calculations (dashed lines) using the FD–FD method of [21].

V. Conclusion

A flexible moment method for the analysis of arbitrary 3-D metallic waveguide N-port structures has been presented. The calculations are based on the EFIE applying the free-space Green's function. The accuracy of the method is verified by measurements or reference values. Its versatility and flexibility is demonstrated by examples of practical importance, including a twisted waveguide structure and a waffle-iron filter with round teeth.

Appendix

A. Equations for Region I

The elements of the waveguide admittance matrix and the excitation matrix are defined as [9]

$$T^I_{pq} = \begin{cases} -\eta_0 \sum_i B_{pi} Y_i A_{iq}, & p \text{ and } q \text{ associated with the same waveguide port} \\ 0, & \text{else} \end{cases} \tag{15a}$$

and

$$I^{\text{inc}}_{pj} = \begin{cases} 2Y_j a^{\text{inc}}_j B_{pj}, & p \text{ and } j \text{ associated with the same waveguide port} \\ 0, & \text{else} \end{cases} \tag{15b}$$

with

$$A_{iq} = \begin{cases} \int_{S_n} \mathbf{M}_q \cdot (\hat{\mathbf{z}} \times \mathbf{e}_i)\, dS, & i \text{ and } q \text{ associated with the same waveguide port } n \\ 0, & \text{else} \end{cases} \tag{15c}$$

and

$$B_{pi} = \begin{cases} \int_{S_m} \mathbf{W}_p \cdot (\hat{\mathbf{z}} \times \mathbf{e}_i)\, dS, & p \text{ and } i \text{ associated with the same waveguide port } m \\ 0, & \text{else,} \end{cases} \tag{15d}$$

where the $\mathbf{e}_i$ are the TE and TM eigenvectors of the waveguides and Y_i is the modal admittance of the mode i. a^{inc}_j is the amplitude of the incident mode j. The summation index i in (15a) considers all modes of the waveguide that is associated with p and q.

The eigenvectors are normalized in the usual way

$$\int_{S_a} \mathbf{e}_i \cdot \mathbf{e}_j\, dS = \delta_{ij} = \begin{cases} 1, & i = j \\ 0, & i \neq j. \end{cases} \tag{16}$$

Acknowledgment

The authors greatly acknowledge the reference calculations by their colleagues R. Lotz and R. Beyer.

References

[1] R. F. Harrington, *Field Computation by Moment Method*. New York: Macmillan, 1968.

[2] H. Auda and R. F. Harrington, "Inductive posts and diaphragms of arbitrary shape and number in a rectangular waveguide," *IEEE Trans. Microwave Theory Tech.*, vol. MTT-32, pp. 606–613, June 1984.

[3] J. M. Jarem, "A multifilament method-of-moments solution for the input impedance of a probe-excited semi-infinite waveguide," *IEEE Trans. Microwave Theory Tech.*, vol. MTT-35, pp. 14–19, Jan. 1987.

[4] X.-H. Zhu, D.-Z. Chen, and S.-J. Wang, "A multistrip moment method technique and its application to the post problem in a circular waveguide," *IEEE Trans. Microwave Theory Tech.*, vol. 39, pp. 1762–1766, Oct. 1991.
[5] O. M. C. P. Filho and L. C. da Silva, "Scattering matrix of cylindrical posts centered on the walls of rectangular waveguides," *IEEE Trans. Microwave Theory Tech.*, vol. 42, pp. 1198–1206, July 1994.
[6] M. S. Leong, L. W. Li, P. S. Kooi, T. S. Yeo, and S. L. Ho, "Input impedance of a coaxial probe located inside a rectangular cavity: Theory and experiment," *IEEE Trans. Microwave Theory Tech.*, vol. 44, pp. 1161–1164, July 1996.
[7] K. Mahadevan and S. Gosh, "Precision analysis of a four-port rectangular orthomode transducer using the method of moments," in *IEEE AP-S Symp. Dig.*, Baltimore, MD, June 1996, pp. 1988–1991.
[8] J. R. Mautz and R. F. Harrington, "A generalized network formulation for aperture problems," *IEEE Trans. Antennas Propagat.*, vol. AP-24, pp. 870–873, MONTH 1976.
[9] H. Auda and R. F. Harrington, "A moment solution for waveguide junction problems," *IEEE Trans. Microwave Theory Tech.*, vol. MTT-31, pp. 515–520, July 1983.
[10] E. Kühn and V. Hombach, "Computer-aided analysis of corrugated horns with axial ring or ring-loaded radial slots," in *Proc. ICAP'83—Part I*, pp. 127–131.
[11] R. E. Collin, *Field Theory of Guided Waves*. New York: IEEE Press, 1991.
[12] T. K. Sarkar, S. M. Rao, and A. R. Djordjevic, "Electromagnetic scattering and radiation from finite microstrip structures," *IEEE Trans. Microwave Theory Tech.*, vol. 38, pp. 1568–1575, Nov. 1990.
[13] U. Jakobus and F. M. Landstorfer, "Novel basis function for the equivalent magnetic current in the method of moments solution of dielectric scattering problems," *Electron. Lett.*, vol. 29, pp. 1272–1273, July 1993.
[14] X. Q. Sheng, J.-M. Jin, J. Song, W. C. Chew, and C.-C. Lu, "Solution of combined-field integral equation using multilevel fast multipole algorithm for scattering by homogeneous bodies," *IEEE Trans. Antennas Propagat.*, vol. 46, pp. 1718–1726, Nov. 1998.
[15] S. M. Rao, D. R. Wilton, and A. W. Glisson, "Electromagnetic scattering by surfaces of arbitrary shape," *IEEE Trans. Antennas Propagat.*, vol. AP-30, pp. 409–418, May 1982.
[16] D. R. Wilton, S. M. Rao, A. W. Glisson, D. H. Schaubert, O. M. Al-Bundak, and C. M. Butler, "Potential integrals for uniform and linear source distributions on polygonal and polyhedral domains," *IEEE Trans. Antennas Propagat.*, vol. AP-32, pp. 276–281, Mar. 1984.
[17] P. C. Hammer, O. P. Marlowe, and A. H. Stroud, "Numerical integration over simplexes and cones," *Math. Tables Aids Comput.*, vol. 10, pp. 130–137, 1956.
[18] J. M. Reiter and F. Arndt, "Rigorous analysis of arbitrarily shaped H- and E-plane discontinuities in rectangular waveguides by a full-wave boundary contour mode-matching method," *IEEE Trans. Microwave Theory Tech.*, vol. 43, pp. 796–801, Apr. 1995.
[19] R. Beyer and F. Arndt, "The generalized scattering matrix separation technique combined with the MM/FE method for the efficient modal analysis of a comprehensive class of 3-D passive waveguide circuits," in *IEEE MTT-S Int. Microwave Symp. Dig.*, Orlando, FL, May 1995, pp. 277–280.
[20] G. L. Matthaei, L. Young, and E. M. T. Jones, *Microwave Filters, Impedance-Matching Networks, and Coupling Structures*. New York: McGraw-Hill , 1964, p. 408.
[21] R. Lotz, J. Ritter, and F. Arndt, "3-D subgrid technique for the finite difference method in the frequency domain," in *IEEE MTT-S Int. Microwave Symp. Dig.*, Baltimore, MD, June 1998, pp. 1739–1742.

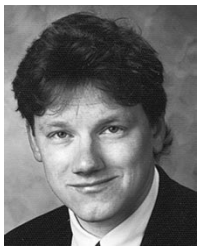

Rainer Bunger (M'93) received the Dipl.-Ing. and Dr.-Ing. degrees from the University of Bremen, Bremen, Germany, in 1992 and 1997, respectively.

In 1998, following a short stay at the Technical University of Darmstadt, Darmstadt, Germany, he continued his involvement on numerical techniques for the solution of electromagnetic-field problems at the University of Bremen. His research interests include the method of moments, the fast multipole method, and the finite-difference time-domain technique.

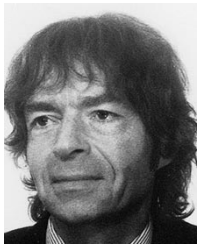

Fritz Arndt (SM'83-F'93) received the Dipl.-Ing., Dr.-Ing., and Habilitation degrees from the Technical University of Darmstadt, Darmstadt, Germany, in 1963, 1968, and 1972, respectively.

From 1968 to 1972, he was a Research Associate at the Technical University of Darmstadt. Since 1972, he has been a Full Professor and Head of the Microwave Department, University of Bremen, Bremen, Germany. He has authored or co-authored over 200 technical papers, mainly in the field of electromagnetic computer-aided design (CAD) of microwave and antenna components. His research interests include numerical methods for the rigorous and fast CAD of waveguide, microwave, millimeter-wave, and optical waveguide circuits, as well as of horn and microstrip antennas. He is also interested in the simulation of mobile communication channels.

Dr. Arndt is a member of the Berein Deutscher Elektroingerieure (VDE) and Nachrichten-Technische-Gesellschaft (NTG), Germany. He is a member of the Editorial Board of the IEEE TRANSACTIONS ON MICROWAVE THEORY AND TECHNIQUES, and he has served on the Technical Program Committee (TPC) of the IEEE International Microwave Symposium and on the TPC of the IEEE European Microwave Conference. From 1993 to 1996, he was chairman of the German IEEE joint Microwave Theory and Techniques Society (IEEE MTT-S) and the IEEE Antennas and Propagation Society (IEEE AP-S) chapter. He received the 1970 NTG Outstanding Publications Award, the 1983 A. F. Bulgin Award (together with three co-authors) presented by the Institution of Radio and Electronic Engineers, and the 1986 Best Paper Award presented at the Antenna Conference Journees Internationales des Antennes (JINA), Nice, France.